Journal of Metals, Materials and Minerals, Vol.28 No.2 pp.11-17, 2018

Plasticity of light metal matrix composites under anodic polarization

Yaakov B. UNIGOVSKI[1,*], Emmanuel M. GUTMAN[1], Zamir KOREN[2], and Haim ROSENSON[2]

[1]*Ben-Gurion University of the Negev, 84105, Beer-Sheva, Israel*
[2]*Israel Institute of Metals, Technion, 32000, Haifa, Israel*

***Corresponding author e-mail:** yakovun@bgu.ac.il

Received date:
18 April 2018
Revised date:
25 April 2018
Accepted date:
30 June 2018

Keywords:
Hardness
Anodic polarization
Al and Mg matrix composites

Abstract

Light metal matrix composites (MMCs), reinforced with ceramic particles, demonstrate an improvement in strength, elasticity, and wear resistance with regards to matrix alloys. Unfortunately, the plasticity of MMCs is rather low, and their hardness is relatively high. Therefore, there are serious problems in formability and machinability of these materials. In the present study, an improvement in the surface plasticity of such light MMCs as Al 6063-10% SiC (AMC) and Mg AZ31-10% SiC (MgMC) as well as the high-strength Al 7075 T6 alloy under anodic polarization was observed. To assess the effect of polarization on plasticity of composites, the relative Vickers hardness (RVH) was used, which was found as the square of the ratio of the depth of penetration of the indenter into the metal in air and in the electrolyte. In the acid electrolyte 0.3 M HCl + 0.6 M NaCl, both composites demonstrated a very intense drop in RVH at low current densities ($\leq$1 mA cm^{-2}), while in tap water a small effect of anodic polarization on the relative hardness was obtained. Corrosion rate of an AMC in 0.6 M NaCl solution was much higher with respect to matrix alloy.

1. Introduction

Substantial progress in the development of light metal matrix composites has been achieved in recent decades into the most important applications, especially in the automotive industry, portable digital devices, etc. Besides, specialty applications in the space shuttle, Hubble telescope, and other systems have been seen [1]. Magnesium and aluminum alloys, which demonstrate good castability and high specific strength, are natural candidates to be used as a metal matrix [2]. Every casting method that can be used with unreinforced alloys has been used with aluminum and magnesium MMCs. These include the sand, permanent mold, squeeze, die casting, etc. Some modifications to the normal casting practice, e.g., stirring, must be made in order to produce high-quality cast composites. SiC particles will concentrate on the bottom of the furnace if the melt is not stirred [1]. Powder metallurgy processing of AMCs and MgMCs involves compacting, and consolidation by vacuum hot pressing or hot isostatic pressing. If it is necessary to deform cast or compacted green billets, they must be hot extruded, rolled or drawn at temperatures between 200°C and 450°C [1-7]. For example, cast billets of MgMCs reinforced with SiC_p produced by stir casting using AZ31 [3] or AZ91 alloy [3,5] were hot extruded at temperatures ranged between 200°C and 350°C. Using powder metallurgy, Witte et al. produced biodegradable MgMC AZ91-20% HA (hydroxyapatite) which was extruded at 400°C to a diameter of 18 mm [6]. Another example was reported by Purohit et al. [7] where green compacts of Mg-SiC_p composites with 10, 20 and 30 wt% of SiC_p were sintered in a solid state at a temperature of 460°C for 30 min.

The addition of ceramic particles to the light alloys has been associated with improvements in strength, elasticity, wears resistance, and sometimes corrosion resistance. Unfortunately, the ductility and fracture toughness of the MMCs are quite low while their hardness is relatively high. Therefore, there are serious problems in formability and machinability of these materials, cold deformation of which is practically impossible. The problems of cold deformation of hard and brittle materials can be overcome in the forming processes assisted by anodic polarization. It was found that plasticization of the metal surface due to chemical/ electrochemical interactions between an electrolyte and metal is caused by the chemomechanical effect (CME, 1967). The CME was explained as destruction of dislocation pile-ups in a strain-hardened surface layer due to chemical or

DOI: 10.14456/jmmm.2018.20

electrochemical interactions between an electrolyte and metal [8,9]. As a result, an additional dislocation flux is generated. It is reported that due to the CME hardness of a 304-type stainless steel in a 3.5 M H_2SO_4 solution decreased linearly with an increase in the logarithm of the anodic current density by more than 40% in comparison with the deformation in the air [8,9]. The same hardness behavior was found for carbon steels AISI 1020 and AISI 1070 as well as FeSi6.5 [10] during anodic dissolution in an acid as well as in potassium and sodium chlorides solutions.

Cold deformation processes assisted by anodic polarization can be called 'electrochemical forming processes'. At electrochemical cold drawing (ECD) of tubes made of a high-strength alloy (25Cr-60Ni-15V), it was found a decrease by 20% in drawing force achieved due to the CME [8]. Recently, it was found that during the ECD of AM60B alloy bars (Mg–6.0% Al)[11] and Mg_2Si_p/AM60B[12], hardness and drawing force significantly decreased in comparison to drawing in air. Compared with the drawing in air, the ECD significantly reduced both the drawing force and surface hardness of the magnesium matrix composite, although the electrochemical plasticization of the MMC was relatively lower than that of the alloy, owing to the presence of Mg_2Si particles.

Corrosion behavior of light composites reinforced by silicon carbide, in particular, in NaCl solutions, has been reported both for AMCs [1,13-16] and MgMCs [17-20]. General corrosion is more significantly affected by the presence of oxygen than by the SiC phase. For aluminum-based composites, in deaerated solutions containing oxygen, corrosion rates of both matrix aluminum alloy and its composite reinforced by SiC were approximately the same [13-16]. However, the effect of SiC on the corrosion potential E_{corr} for three composite systems: SiC/A1 2024, SiC/A1 6061, and SiC/A1 5456 is not as clear [14]. The addition of SiC to these alloys can result in E_{corr} being more positive, more negative, or unchanged, depending on the alloy system and on deaeration conditions. The SiC phase does not affect the susceptibility to pit initiation of the composites tested, except for A1 2024. In this system, the composite is somewhat more susceptible to pit initiation than the matrix alloy [14]. As the oxidation product, aluminum hydroxide is formed which does not dissolve and precipitates as a white gelatinous mass, commonly referred to as alumina, although, as a rule, it is bayerite (β-$Al_2O_3{\cdot}3H_2O$). It was also found that with increased exposure time, the corrosion rate is decreased due to formation of boehmite (AlO.OH) [15,17]. The magnesium alloys and their composites reinforced with silicon carbide, exhibit two-three orders of magnitude higher values of CR, than those obtained for aluminum alloys [17-20].

In magnesium-based MMCs, SiC particles usually do not cause galvanic corrosion, however, higher corrosion rates of composites may be related to the defective nature of the Mg/SiC interfaces [18-20]. Besides, the SiC particles cause detrimental effect on the continuity of the β-phase [20]. Corrosion products can be represented, mainly, by hydroxide $Mg(OH)_2$ [18] and, e.g., by $(Mg, Al)_n(OH)_m$ in Mg-9Al-based alloys [18,21,22].

Thus, the cold deformation of MMCs, particularly by cold drawing using traditional lubricants, is practically impossible. Only electrochemical forming, as indicated above for electrochemical drawing, can reduce the hardness of the surface layer during electrochemical interactions between deformed metal and electrolyte. Recently published work by Li et al. [12] on the electrochemical cold drawing of a MgMC (Mg-6%Al alloy with in situ Mg_2Si particles) demonstrates a decrease in microhardness after drawing assisted with anodic polarization of the rod. However, the effect of such polarization of other MgMCs, especially, those reinforced by silicon carbide, on their plasticity has not been investigated. Corrosion behavior of Al6063-10% SiC_p alloy has not been also studied.

In this research, the effect of in situ anodic polarization of the magnesium (MgMC) and aluminum (AMC) matrix composites reinforced by 10 wt% silicon carbide particles as well as high-strength Al 7075 T6 alloy on Vickers microhardness was investigated. In addition, corrosion behavior of Al6063/SiC_p system was studied.

2. Experimental

The Al 7075 T6 alloy, AMC (Al 6063 -10% SiC_p) and MgMC (AZ31 -10% SiC_p) were studied (Table 1). In brief, the procedure for obtaining composite alloys is as follows [3]: melting of the base alloy; preliminary heating of SiC particles at 600°C for 1 h; vigorously stirring of molten metal with decreasing temperature; adding particles to the melt in a semi-solid state at a temperature of 10°C below the liquidus line; stirring the melt for 2 h; and,

finally, semi-solid casting at a temperature of 15°C below the liquidus line. In order to avoid segregation of the components during the casting due to the significant difference in the specific densities of materials, the SiC particles (15-30 μm) were added in a continuously stirred melt. Observation of the microstructure showed a homogenous distribution of particles in the cast matrix of both MMCs. Figure 1 shows, as an example, a SEM micrograph of an AZ31 specimen with 10wt% of SiC particles.

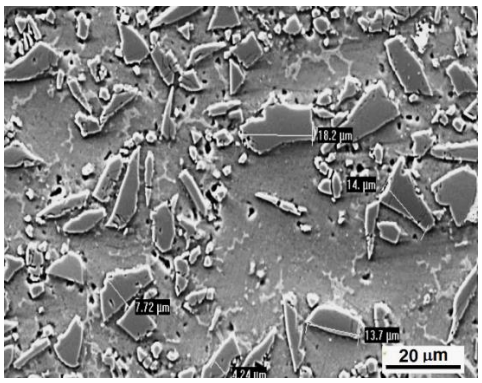

Figure 1. SEM photomicrograph of MgMC showing particles of silicon carbide in the cast matrix of AZ31 alloy.

Hardness is inversely proportional to the imprint area or to the squared indentation depth. Therefore, a squared ratio of the penetration depth $(h_{air}/h_{sol})^2$, i.e., RVH = $(h_{air}/h_{sol})^2$ can be used as a parameter of the relative Vickers hardness (RVH) in solution as compared to that in air. The microhardness of the alloys was studied on a Vickers tester (Zwick Co., Germany) equipped with an AC/DC power supply ZUP36-24 and a transparent electrochemical cell allowing local plastic deformation of the metal with simultaneous anodic polarization of a sample having a dissolution area of 0.5 cm^2. As a cathode was the platinum wire ring, in the center of which was placed a 90°cone-shaped indenter made of tungsten carbide-cobalt alloy. Hardness measurements in air and in solutions under anodic polarization were performed using this indenter under a load of 2.9 N. The penetration of the indenter in the sample both in air and in electrolytes was several tens of microns. The magnitude of the anode current ranged from 0.02 to 20 mA and was generally constant when measuring the hardness that was provided by a power source and a variable resistance reference connected in series with the resistance of the liquid electrolyte between the anode (alloy) and the platinum cathode. As electrolytes were used 0.3 M HCl + 0.6 M NaCl (pH 1.6) solution and tap water (pH ≈ 6). The experimental setup and method have been described in detail previously [10]. The hardness of materials, measured at load of 2.9 N, was 1.71 GPa, 1.08 GPa and 0.76 GPa for 7075 Al, AMC and MgMC, respectively.

The corrosion behavior of Al 6063/10% SiC_p was investigated by potentiodynamic polarization in a three-electrode cell using the Bio-Logic SP-200 potentiostat equipped with EC-Lab® V10.44 software. The cell included the alloy as a work electrode, the reference saturated calomel electrode (SCE), and the Pt counter electrode. To compare the corrosion resistance of the matrix and AMC, 0.6 molar sodium chloride solution (3.5% NaCl) was chosen, since the behavior of metals in this medium is the most studied. The solution was quiescent and opened to the air. The samples with a reaction surface area of 1.0 cm^2 were ground with grit SiC papers (grade 320, 600 and 800), then washed in water and ethanol and ultrasonically cleaned in acetone for 5 min. The working electrode was immersed in the solution at for 15 min before measurement in order to attain a steady state condition and fixation of open circuit potential (OCP). Corrosion potential and corrosion rate were found by Tafel approximation of cathodic and anodic branches of polarization diagrams. A potential range from -1.2 V up to +0.2 V was used with the sweep rate of 1.0 mV/s.

Microstructure of composites was studied by a model Jeol JSM-35CF scanning electron microscope with a ‘‘Link system’’ AN 10,000 energy dispersive spectroscope.

Table 1. Chemical composition of materials, wt%.

Material	Zn	Si	Cu	Cr	Mg	Al	Density, g/cm^3
Al 7075	5.8	<0.5	1.6	0.2	2.4	balance	2.8
Al 6063	<0.1	0.4	<0.1	<0.1	0.6	balance	2.7
AZ31	1.1	<0.05			balance	3.2	1.8
	C	Si	SiO_2	Fe_2O_3	Al_2O_3	SiC	
SiC_p	0.40	0.60	0.75	0.05	0.20	balance	3.2

3. Results and discussion

The duration of hardness measurements in the solution, as a rule, does not exceed 12 min (Figure 2). The application of anode current during the test is not accompanied by a noticeable precipitation of oxides on the surface, since during this short time active dissolution of elements is accompanied by the transfer of cations to the solution.

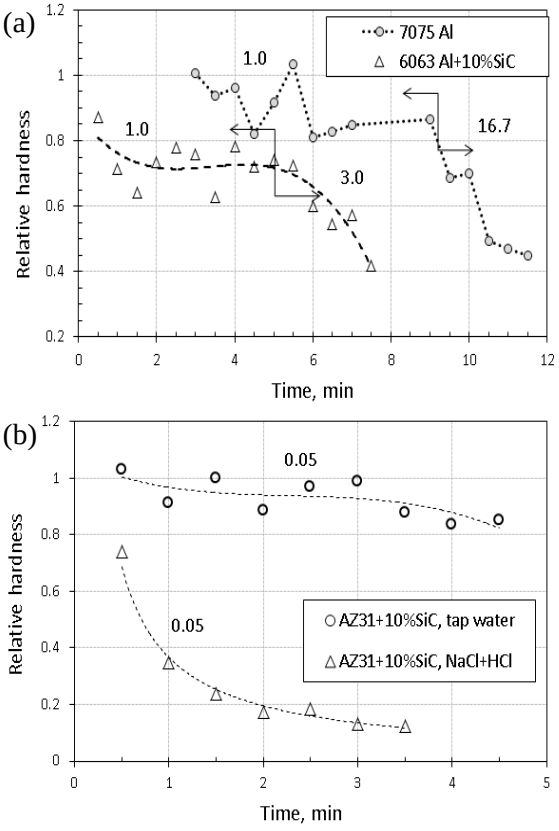

Figure 2. The time dependent relative hardness of 7075Al alloy (a), 6063 Al + 10% SiC (a) and AZ31+10% SiC (b) in 0.3 M HCl + 0.6 M NaCl solution (a, b) and tap water (b) under anodic polarization (the numbers on the curves are the current density *j*, mA cm^{-2}).
The arrows pointing in opposite directions indicate a jump *j*.

The effect of anodic polarization on relative hardness in the acid electrolyte 0.3 M HCl + 0.6 M NaCl is much more pronounced for AMC in comparison with 7075 Al alloy even at a low current density *j* that was 1.0 mA cm^{-2} (Figure 2a). Almost 17-fold jump of *j* for 7075 Al, and three-fold *j* jump for the AMC resulted in a significant decrease in hardness RVH of surface layer under anodic polarization up to about 0.4 or by 60% (Figure 2a). In the same acid electrolyte, MgMC demonstrates very intense drop in RVH even at ultralow current density (0.05 mA cm^{-2}), however, the composite shows a negligible effect in tap water (Figure 2b).

In materials science, plasticity of a metal describes the deformation of a material undergoing non-reversible changes of shape in response to applied forces when a material is stressed above its elastic limit. Plasticity or deformation ability of materials can be characterized by hardness measurements. During the hardness test, the indenter causes plastic deformation of the metal under applied weight. Therefore, there is a direct relationship between the hardness and plasticity of the material.

The freshly ground surface of the alloys is covered with a thin layer of oxides. The indenter immersed in the electrolyte penetrates into the metal through the oxide layer to a depth of several tens of microns, depending on the current density, the type of alloy and the composition of the electrolyte. Ions of magnesium Mg^{2+} and aluminum Al^{3+} have a much smaller ionic radius compared to hydroxyl OH^-, namely 86, 67.5 and 110 picometers, respectively [23]. Therefore, when the polarization potential is applied to the surface of the alloy in contact with the electrolyte, small cations of Mg^{2+} and Al^{3+} penetrate the film of the natural oxide outward to the hydroxyl ions, and then magnesium or aluminum hydroxides precipitate. On the surface of the Mg-9% Al alloy, e.g., there is an oxide film with a thickness of up to 150 nm, which consists of MgO, $Mg(OH)_2$ and $Al(OH)_3$, as well as the inclusions of the metallic phase [18,22]. The native oxide film present on aluminum surfaces, which is typically less than a few tens of nanometers thick in air, turns into boehmite ($\alpha-Al_2O_3.H_2O$) after exposure to an aqueous solution [24,25]. In contrast, as mentioned above [15,17], boehmite is formed only after a long exposure of the alloy in NaCl solution.

The presence of a thin electrolyte film between the indenter and the alloy substrate when measuring hardness can lead to a decrease in frictional force and an increase in penetration depth. However, as reported in [10] for steel wire AISI 1055, the effect of the electrolyte on the hardness value is insignificant compared to measurements in air when the anodic polarization is absent. This steel shows a decrease in hardness in 3.5 M chloric and sulfuric acids compared to air by 8% and 11%, respectively.

Thus, a noticeable decrease in the relative hardness of aluminum- and magnesium-based

composites and a strong aluminum alloy 7075 under polarization in the 0.3 M HCl + 0.6 M NaCl electrolyte was observed. Hardness measurements with simultaneous anodic polarization were studied as mentioned above for stainless steel [8], carbon and silicon steels [10]. Such data for other alloys and MMCs are absent. Nevertheless, Li et al. [11,12] reported a post-effect associated with a decrease in the hardness of bars made of AM60 and AM60-Mg_2Si after their cold drawing under anodic polarization in various electrolytes. For example, Vickers hardness of AM60-Mg_2Si bars drawn in 0.3 M HCl + 0.6 M NaCl decreased from 112 to 95 HV with increasing current density from 3.0 to 8.5 mA cm^{-2} [12]. As reported in this paper, the drawing speed is the dominant parameter affecting the hardness after drawing. When the MgMC bars were produced using the regular and electrochemical drawing, the hardness of the alloy drawn at the lowest rate of 0.12 m s^{-1} was 110 and 90 HV, respectively (-18%). As the drawing speed increases, the efficiency of the ECD process decreases. The results of electrochemical cold drawing of thin-walled stainless steel pipes [8], as well as magnesium alloy bars AM60 [11] and composite AM60-Mg_2Si [12] confirm the positive effect of anodic polarization of the metal on the increase in its plasticity, which is expressed in the reduction of drawing force. Investigation of corrosion behavior of Al 6063, Al 6063 alloys and Al 6063-10% SiC_p composite in 0.6 M NaCl using potentiodynamic polarization at room temperature showed an appreciable shift of cathodic and anodic curves in the direction of increasing current density for Al 7075 (Figure 3). Corrosion potentials for Al 7075, Al 6063 and Al 6063+10%SiC amounted to -0.770, -0.723 and -0.698 V, respectively. The shift of the corrosion potential in Al 6063-10% SiC as compared with the matrix alloy in the more positive region from -0.723 V to -0.698 V is probably related to the non-reactivity of the part of the material (SiC_p) with the corrosion solution. A similar behavior of the 2024 Al -20% SiC alloy in 0.1 M NaCl solution was found by McCafferty and Trzaskoma (1981) as reported in an earlier review [13] as well as in Al 2014 +(10-25)%SiC [17].However, Shimizu et al [16] found that both the Al 6061 and the Al 6061 -20% SiC_w (SiC whiskers) demonstrated practically the same corrosion and pitting potentials under polarization in 3.5% NaCl solution.

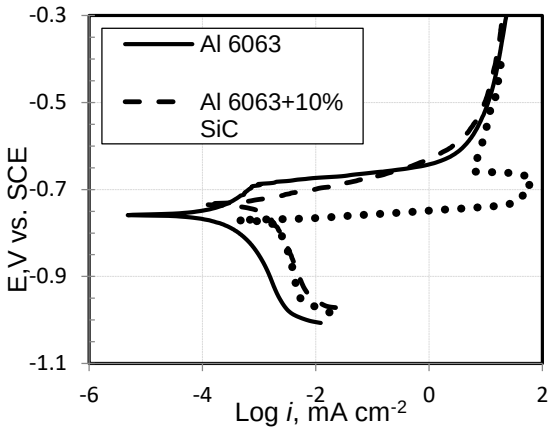

Figure 3. Potentiodynamic polarization curves for Al alloys Al 6063, Al 7075 and Al 6063+10% SiC in 0.6 M NaCl solution at room temperature.

With the growth of the working electrode potential in the anode region from -0.723 V (corrosion potential) to 0.692 V (pitting potential), the matrix alloy 6063 demonstrates an increase in the anode current, the magnitude of which sharply increases with the formation of pit (Figure 3). Meanwhile, a composite based on this alloy does not show a similar jump of current. Note that this last result may reflect a matrix microstructure of the composite different from the extruded matrix alloy.

The Tafel approximation showed that corrosion rates (CRs) for Al 7075, Al 6063 and Al 6063-10% SiC_p alloys in 0.6 M NaCl solution at room temperature amounted to $37.6x10^{-3}$, $4.3x10^{-3}$ and $21.8x10^{-3}$ mmpy (mm $year^{-1}$), respectively. Nonmetallic inclusions in Al 7075 are usually represented by $Mg(Zn_2AlCu)$, Mg_2Si, $(Fe, Cr)_3SiAl_{12}$ etc., and in Al 6063 – by Mg_2Si [26]. Since Al 7075 contains much more precipitations than Al 6063, the development of galvanic corrosion between the active matrix and the more noble precipitations causes an almost nine times higher corrosion rate of Al 7075 compared to Al 6063. On the other hand, the Al 6063-10% SiC showed a fivefold increase in CR as compared to its matrix alloy.

The SiC is an insulator and is not expected to have any galvanic interaction with the Al 6063 matrix. However, it was likely that the reinforcement increased the corrosion rate due to the presence of Al matrix/SiC_p interfaces breaking the continuity of the Al matrix and creating preferential locations for corrosion attack. Moreover, according to the cathodic branches of the polarization curves, higher cathodic currents are

found when adding the SiC_p to Al 6063; this evidences that galvanic corrosion at the SiC/Al interface is likely to occur in the studied composite.

As to the effect of silicon carbide particles on the corrosion of Mg MMC, the literature almost unambiguously indicates that an increase in SiC leads to an increase in the corrosion rate of MMC [18-20]. In this study, the corrosion of the AZ31-SiCp composite in a solution of sodium chloride was not investigated. However, we can estimate the effect of an 10% SiC_p additive on CR of AZ31-based composite. It was reported for extruded Mg alloys AZ31 and AZ92 (Mg-9Al-2Zn) that the values of CR in 0.6 M NaCl amounted to 3.8 mmpy [27] and 2.0 mmpy [21], respectively. It is found that CR increases from 2.0 to 2.7 mmpy when adding the 10% SiC_p to AZ92 alloy in 0.6 M NaCl [21]. Tiwari et al. [19] found that the CR for extruded Mg - 6 vol% SiC composite in 1 M NaCl amounts to 18 mmpy. Thus, the extruded magnesium alloys and their composites reinforced with silicon carbide, exhibit three orders of magnitude higher values of CR, than those obtained for aluminum alloys.

The duration of contact of the metal with the electrolyte does not exceed one fifth of 1 h. With uniform corrosion for the specified time, the thickness of the layer of the material removed from the surface of the working electrode does not exceed $1x10^{-3}$ micrometer for aluminum alloys, and about 0.3 microns for a MgMC [21]. Since the penetration of the indenter into the studied Al and Mg composites was several tens of microns, the influence of anodic dissolution of Al and Mg on the accuracy of hardness measurements can be neglected in the first approximation.

Thus, a significant reduction in the relative hardness of Al 6063 and AZ31 alloys reinforced with carbide particles, as well as a strong aluminum alloy 7075, under anodic polarization in the acid electrolyte confirms the previously obtained results on steels. The plasticity of materials under cold deformation can be increased by simultaneous anodic polarization.

4. Conclusions

Thus, a plasticization of the surface layer as a result of anodic electrochemical polarization was found for 7075 Al alloy as well as for Mg- and Al-based MMCs. The follow conclusions can be done:

- Since Al 7075 contains much more precipitations than Al 6063, the development of galvanic corrosion between the matrix and the more noble non-metallic inclusions causes a nearly 9-fold higher corrosion rate of Al 7075 compared to Al 6063.
- In the acid electrolyte 0.3 M HCl + 0.6 M NaCl, the plasticization effect is much more pronounced for 6063Al -10% SiC_p in comparison with 7075 Al alloy even at low current density (1.0 mA cm^{-2}). In the same solution, MgMC demonstrates a very intense drop in RVH at an ultra-low current density (0.05 mA cm^{-2}), while in tap water a slight effect of anodic polarization on the relative hardness is found.
- Composite 6063-10% SiC exhibits a fivefold increase in CR compared with its matrix alloy. When SiC_p is added to Al 6063, a higher cathode current is detected; this indicates that in the composite, galvanic corrosion is likely to occur at the SiC_p/Al interface.

References

[1] ASM Handbook, Vol. 21(2001): Composites, D. B. Miracle and S. L. Donaldson, eds., pp. 2341-2387.

[2] K. U. Kainer, “Basics of Metal Matrix Composites,” in: *Metal Matrix Composites. Custom-made Materials for Automotive and Aerospace Engineering.* Ed. by Kainer, WILEY-VCH Verlag, Weinheim, 2006, pp.1-54.

[3] Z. Koren, H. Rosenson, and E. M. Gutman, “Development of die-cast magnesium matrix reinforced by SiC particles,” Proceed. 11th European Conference on Composite Materials, Rhodes, Greece, May 31 – June 3, 2004.

[4] M. J. Shen, M. F. Zhang, and W. F. Ying, “Processing, microstructure and mechanical properties of bimodal size SiC_p reinforced AZ31B magnesium matrix composites,” *Journal of Magnesium and Alloys*, vol. 3, pp.162-167, 2015.

[5] X. J. Wang, L. Xu, X. S. Hu, K. B. Nie, K. K. Deng, K. Wu, and M. Y. Zheng, “Influences of extrusion parameters on microstructure and mechanical properties of particulate reinforced magnesium matrix composites,”

Materials Science and Engineering A, vol.528, pp. 6387– 6392, 2011.

[6] F. Witte, F. Feyerabend, P. Maier, J. Fischer, M. Stoermer, C. Blawert, W. Dietzel, and N. Hort, "Biodegradable magnesium–hydroxyapatite metal matrix composites," *Biomaterials*, vol. 28, pp. 2163–2174, 2007.

[7] R. Purohit, Y. Dewang, R. S. Rana, D. Koli, and S. Dwivedi, "Fabrication of magnesium matrix composites using powder metallurgy process and testing of properties," *Materials Today: Proceedings*, vol. 5, pp. 6009–6017, 2018.

[8] E. M. Gutman, *Mechanochemistry of Solid Surfaces*. World Sci. Publish.: New Jersey, pp. 322, 1994.

[9] E. M. Gutman, "Surface plasticity modification using electrolytic etching," *Surface Coating Technology*, vol. 67, pp. 133–136, 1994.

[10] E. M. Gutman, Y. Unigovski, R. Shneck, F. Ye, and Y. Liang, "Electrochemically enhanced surface plasticity of steels," *Applied Surface Science*, vol. 388, pp. 49–56, 2016.

[11] L. Li, T. Chen, S. Zhang, E. M. Gutman, Y. Unigovski and F. Yan, "Electrochemical cold drawing of Mg alloy bars," *Materials Science and Technology*, vol. 33, pp. 244-254, 2017.

[12] L. L. Li, T. J. Chen, S. Q. Zhang, and F. Y. Yan, "Electrochemical cold drawing of in situ Mg2Sip/AM60B composite: A comparison with the AM60B alloy," *Journal Mater Process Technol*, vol. 240, pp. 33-41, 2017.

[13] M. Metzger and S. G. Fishman, "Corrosion of Aluminum - Matrix Composites. Status Report," *Ind. Eng. Chem., Prod. Res. Dev.*, vol. 22, pp. 296-302, 1983.

[14] P. P. Trzaskoma, E. McCafferty, and C. R. Crowe, "Corrosion Behavior of SiC/Al Metal Matrix Composites," *J. Electrochem. Soc.: Electrochemical, Science and Technology*, vol. 130, pp. 1804-1809, 1983.

[15] A. S. Verma, Sumankant, N. M. Suric, Yashpal, "Corrosion Behavior of Aluminum base Particulate Metal Matrix Composites: A review," *Materials Today: Proceedings*, vol. 2, pp. 2840 – 2851, 2015.

[16] Y. Shimizu, T. Nishimura, and I. Matsushima, "Corrosion resistance of Al-based metal matrix composites," *Material Science Engineering A*, vol. 198, pp. 113-118, 1995.

[17] I. B. Singh, D. P. Mandal, M. Singh, and S. Das, "Influence of SiC particles addition on the corrosion behavior of 2014 Al–Cu alloy in 3.5% NaCl solution," *Corrosion Science*, vol. 51, pp. 234–241, 2009.

[18] M. Esmaily, J. E. Svensson , S. Fajardo, N. Birbilis, G. S. Frankel, S. Virtanen, R. Arrabal, S. Thomas, and L. G. Johansson, "Fundamentals and advances in magnesium alloy corrosion," *Progress in Materials Science*, vol. 89, pp. 92–193, 2007.

[19] S. Tiwari, R. Balasubramaniam, and M. Gupta, "Corrosion behavior of SiC reinforced magnesium composites," *Corrosion Science*, vol. 49, pp. 711–725, 2007.

[20] B. Mingo, R. Arrabal, M. Mohedano, A. Pardo, and E. Matykina, "Corrosion and wear of PEO coated AZ91/SiC composites," *Surface & Coatings Technology*, vol. 309, pp. 1023–1032, 2007.

[21] A. Pardo, S. Merino, M. C. Merino, I. Barroso, M. Mohedano, R. Arrabal, and F. Viejo, "Corrosion behaviour of silicon–carbide-particle reinforced AZ92 magnesium alloy," *Corrosion Science*, vol. 51, pp. 841–849, 2009.

[22] Y. B. Unigovski and E. M. Gutman, "Surface morphology of a die-cast Mg alloy," *Applied Surface Science*, vol. 153, pp. 47–52, 1999.

[23] L. Pauling, *The Nature of the Chemical Bond, An Introduction to Modern Structural Chemistry*, (3rd Ed.). Ithaca, NY: Cornell University Press, p. 664, 1960.

[24] R. K. Hart, "The formation of films on aluminum immersed in water," *Trans. Faraday Soc.*, vol. 53, pp. 1020-1027, 1957.

[25] J. K. Thomas and R. S. Ondrejcin, "An evaluation of the thickness and emittance of aluminum oxide films formed in low-temperature water," *Journal of Nuclear Materials*, vol. 199, pp. 192-213, 1993.

[26] ASM Handbook, vol. 9, *Metallography and Microstructures*, Aluminum alloys, Ed.: G. F. Vander Voort, 1994, pp. 351-388.

[27] H. N. Vatan, R. Ebrahimi-kahrizsangi, and M. Kasiri-asgarani, "Structural, tribological and electrochemical behavior of SiC nanocomposite oxide coatings fabricated by plasma electrolytic oxidation (PEO) on AZ31 magnesium alloy," *Journal of Alloys and Compounds*, vol. 683, pp. 241-255, 2016.